

## THE IONIZATION STRUCTURE OF PLANETARY NEBULAE

## I. PURE HYDROGEN NEBULAE

*D. G. Hummer and M. J. Seaton*

(Received 1962 September 26)

*Summary*

The problem is formulated in terms of the equations of radiative transfer, of ionization equilibrium and of the thermal balance.

The intensity of ionizing radiation is  $I_\nu = I_\nu^s + I_\nu^d$ , where  $I_\nu^s$  is the attenuated intensity of stellar radiation and  $I_\nu^d$  the intensity of diffuse radiation produced in the nebula.

In *Approximation I* it is assumed that there is no transfer problem for the diffuse radiation, emission and absorption occurring at the same place. The problem is then solved using a method due to Zanstra and de Jong. Assuming the star to radiate as a black body, numerical results are obtained for a wide range of star temperatures.

In *Approximation II* the transfer equation for  $I_\nu^d$  is solved using the source function from Approximation I. For an isothermal plane parallel model it is found that the mean intensities  $J_\nu$ , as given by Approximations I and II, never differ by more than a few per cent.

---

1. *Introduction.*—This is the first of a series of papers in which we attempt to calculate the ionization equilibrium at all points in a planetary nebula, given the radiation field of the central star. Our results should provide improved information about the structure of nebulae and about the central star radiation fields. The main source of difficulty is that we have coupled equations for the transfer of ionizing radiation, for the ionization equilibrium and for the thermal balance. We consider first the simplest case, that of a pure hydrogen nebula, in order to examine the methods which may be used. Many previous papers have dealt with this problem; we mention those of Ambarzumian (1932), Chandrasekhar (1935), Hagiwara (1938), Strömberg (1939), Aller, Baker and Menzel (1939), Zanstra (1951), de Jong (1951) and Pottasch (1960). For a general review of problems of planetary nebulae we refer to the article by Seaton (1960).

The physical processes in gaseous nebulae are determined by absorption of stellar quanta with frequency  $\nu > \nu_1$ ,  $\nu_1$  being the frequency of the Lyman limit. Most of the basic physics has been worked out long ago by Zanstra (1927, 1931). The problem of the structure of nebulae, considered in the present papers, is similar to the problem considered by Aller, Baker and Menzel (1939). They obtained solutions using a rather elaborate iterative method in which the Eddington approximation was used for the diffuse radiation, that is, the radiation with  $\nu > \nu_1$  produced in the nebula. Numerical results were obtained for a model with an optical depth  $\tau = 3$  at  $\nu = \nu_1$  and a central star radiating as a black body at 80,000 °K.

Our results show that such a nebula will absorb only about 50 per cent of the stellar quanta having  $\nu > \nu_1$ . The idea that planetary nebulae may absorb completely all stellar quanta with  $\nu > \nu_1$  is assumed in Zanstra's method of determining star temperatures, but it appears to be Strömgren (1939) who first estimated the sizes of ionized regions assuming complete absorption. Strömgren made a number of approximations which are not really necessary; thus, in place of the exact equation for the ionization equilibrium, he used a modified form of the equation for thermo-dynamic equilibrium and in treating the structure of the transition region at the outer boundary of a nebula he considered only the case of monochromatic radiation with frequency  $\nu = \nu_1$ . We shall show that black body radiation gives transition regions which are a good deal less sharp. A more accurate formula for the size of the ionized region, given in the present paper, has been compared with Strömgren's formula in the paper by Seaton (1960).

In 1951, Zanstra proposed that, in calculating the ionization structure of nebulae, it would be a good approximation to consider that the diffuse radiation produced at a given point is re-absorbed at the same point. This we refer to as Approximation I. Some numerical results in this approximation were obtained by de Jong (1951). In the present paper we develop the method further and give much more accurate and extensive tabulations of the various functions required. We treat Approximation I as the first approximation in an iterative method of solution. Going to a second approximation shows that Approximation I gives results which are correct to within a few per cent.

The condition of energy conservation may be expressed in a variety of different ways. One approach is to consider the flux of radiant energy, integrated over all frequencies. We find it much more convenient, following Spitzer (1948), to consider the balance of electron kinetic energy. We take account of all radiative processes and, implicitly, we take account of the elastic collision processes effective in setting up Maxwell distributions. The role of inelastic collisions, in a pure hydrogen nebula, is considered in Paper II of the present series (Hummer 1963). Later papers will be concerned with nebulae containing heavy elements as well as hydrogen.

## 2. Formulation

2.1. *The transfer equation for radiation in the Lyman continuum.*—This is

$$\frac{dI_\nu}{dl} = -\kappa_\nu I_\nu + j_\nu \quad (2.1)$$

where  $I_\nu$  is the photon intensity ( $I_\nu d\nu$  photons  $\text{cm}^{-2} \text{sec}^{-1}$  per unit solid angle),  $\kappa_\nu$  the absorption coefficient per unit volume and  $j_\nu d\nu$  the photon emission rate per unit volume per unit solid angle. The element of pathlength is  $dl$ .

The absorption coefficient is

$$\kappa_\nu = N_H a_{1,\nu} \quad (2.2)$$

where  $N_H$  is the number of ground state H atoms per  $\text{cm}^3$  and  $a_{1,\nu}$  is the ground state photo-ionization cross section. We make the assumption, which is certainly justified, that the number of ground state atoms is much larger than the number in excited states. For the photo-ionization cross section we put

$$a_{1,\nu} = Af_\nu \quad (2.3)$$

where  $A = a_{1, \nu_1}$  is the threshold cross section,  $\nu_1$  being the Lyman threshold frequency. Evidently  $f_{\nu_1} = 1$ . The exact expression for  $f_\nu$  is

$$f(y) = y^{-4} \{1 - \exp[-2\pi/(y-1)^{1/2}]\}^{-1} \exp[4 - 4(y-1)^{-1/2} \tan^{-1}(y-1)^{1/2}] \quad (2.4)$$

and the Kramers approximation is

$$f_{\text{Kramers}}(y) = y^{-3}, \quad (2.5)$$

where  $y = \nu/\nu_1$ . We shall use the exact expression for  $f_\nu$  and the exact value of  $A$ ,

$$A = 6.30 \times 10^{-18} \text{ cm}^2. \quad (2.6)$$

We assume that the electrons have a well-defined kinetic temperature,  $T_e$ , and that this is such that

$$kT_e \ll h\nu_1. \quad (2.7)$$

When this condition is satisfied, it may be considered that the only emission of radiation with  $\nu \geq \nu_1$  is that resulting from ground state recombinations,



The emissivity is

$$j_\nu = \frac{\alpha_{1, \nu}(T_e) N_e N_+}{4\pi}, \quad (2.9)$$

where  $N_e$  is the number of electrons per  $\text{cm}^3$ ,  $N_+$  the number of protons and (Milne, 1924)

$$\frac{\alpha_{1, \nu}(T_e)}{4\pi} = 2 \left(\frac{\nu}{c}\right)^2 \left(\frac{h^2}{2\pi m k T_e}\right)^{3/2} a_{1, \nu} \exp[h(\nu_1 - \nu)/kT_e]. \quad (2.10)$$

The number of ground-state recombinations, per  $\text{cm}^3$  per second, is  $\alpha_1 N_e N_+$  where

$$\alpha_1 = \int_{\nu_1}^{\infty} \alpha_{1, \nu} d\nu. \quad (2.11)$$

From the expressions for  $\kappa_\nu$  and  $j_\nu$  we obtain the source function

$$\frac{j_\nu}{\kappa_\nu} = \frac{N_e N_+}{N_H} \left(\frac{h^2}{2\pi m k T_e}\right)^{3/2} 2 \left(\frac{\nu}{c}\right)^2 \exp[h(\nu_1 - \nu)/kT_e]. \quad (2.12)$$

We have neglected stimulated emission. For planetary nebulae this is justified by the fact that the mean photon intensity,

$$J_\nu = \frac{1}{4\pi} \int I_\nu d\omega \quad (2.13)$$

is less than the Planck function for photon intensities,

$$\mathcal{B}_\nu(T_e) = 2 \left(\frac{\nu}{c}\right)^2 [\exp(h\nu/kT_e) - 1]^{-1}, \quad (2.14)$$

by a factor of order  $10^{-13}$ , this being the geometrical dilution factor.

2.2. *The ionization equation.*—This is obtained on equating the number of photo-ionizations from ground-state atoms to the number of radiative recombinations on all states. The equation is

$$4\pi \int \kappa_\nu J_\nu d\nu = N_e N_+ \sum_{n=1}^{\infty} \alpha_n(T_e), \quad (2.15)$$

where the coefficients  $\alpha_n$ , for recombination to level  $n$ , may be evaluated from expressions of the form

$$\alpha_n = \int_{\nu_n}^{\infty} \alpha_{n,\nu} d\nu, \quad (2.16)$$

$\nu_n$  being the threshold frequency for ionization from level  $n$ . Tables for the calculation of  $\alpha_n$  are given by Seaton (1959).

Other possible ionization processes may be mentioned. Collisional ionization from ground-state atoms is generally negligible for  $kT_e \ll h\nu_1$ , but this is readily checked once solutions have been obtained for any particular case. The possible importance of photo-ionization from  $n=2$  is more difficult to settle from a theoretical study, since this depends on the number of atoms in  $n=2$ , as determined from the solution of the Ly $\alpha$  transfer problem, but the question may be settled observationally (Gershberg 1961; Mathis 1962). It appears that the optical depths for the lower Balmer lines, even if appreciable at all, are certainly not very large. The optical depths in the Balmer continuum will be much less than those in the lower Balmer lines and it may therefore be concluded that photo-ionizations from  $n=2$  may be neglected.

2.3. *The energy balance.*—The equations for radiative transfer and for the ionization equilibrium involve the electron temperatures  $T_e$ . This is obtained from the equation for the energy balance, which we express in terms of the balance of electron kinetic energy (Spitzer 1948). Consistent with the assumptions already made, this equation is obtained on equating the kinetic energy gain in ground state photo-ionizations to the loss which takes place on recombinations and in free-free transitions. The equation is

$$4\pi \int \kappa_\nu J_\nu h(\nu - \nu_1) d\nu = N_e N_+ kT_e \left\{ \sum_{n=1}^{\infty} \beta_n(T_e) + \beta_{ff}(T_e) \right\}, \quad (2.17)$$

where  $N_e N_+ kT_e \beta_n$  is the kinetic energy loss, per cm<sup>3</sup> per second, due to recombinations on level  $n$  and  $N_e N_+ kT_e \beta_{ff}$  is the loss due to free-free transitions. The coefficients  $\beta_n$  are obtained from expressions of the form

$$kT_e \beta_n = \int_{\nu_n}^{\infty} \alpha_{n,\nu} h(\nu - \nu_n) d\nu. \quad (2.18)$$

Tables for the calculation of  $\beta_n$  and  $\beta_{ff}$  are given by Seaton (1959, 1960).

For a nebula containing heavier elements, such as oxygen, the equation for the energy balance would include an additional term to allow for the loss of electron kinetic energy in excitation of forbidden lines. The effect of this term will be to make  $T_e$  smaller and more nearly constant throughout a nebula. Collisional excitation plays the same role in a pure hydrogen nebula; this mechanism will be considered in detail in the next paper in the series. In the present paper we shall consider both the case in which  $T_e$  is determined from equation (2.17) and the case in which  $T_e$  is assumed to be constant.

2.4. *Dynamics.*—The equations (2.1), (2.15) and (2.17) enable the intensity,  $I_\nu$ , the ionization equilibrium,  $N_H/N_e N_+$ , and the temperature,  $T_e$ , to be determined as functions of an optical depth variable. To complete the solution of the problem, it is necessary to know how the total hydrogen density  $N = N_+ + N_H$  varies with position. This is determined by dynamical equations. The dynamical problems involve complicated shock-wave phenomena, discussed by Goldsworthy (1961, a and b) and Axford (1961).

Another approach is to appeal to observational evidence. From the observed surface brightness as a function of position on the disc, one may deduce the emission per unit volume on making some assumptions about the symmetry of the nebula, and hence obtain  $N_e N_+$  as a function of position.

The problem which we set ourselves is to solve equation (2.1), (2.15) and (2.17). Having done this, we obtain some simple models based on assumed variations of  $N$  with position.

3. *Approximation I.*—We put

$$I_\nu = I_\nu^s + I_\nu^d \quad (3.1)$$

where  $I_\nu^s$  is the attenuated intensity of stellar radiation and  $I_\nu^d$  is the intensity of diffuse radiation produced in the nebula. Within the nebula there is no source of  $I_\nu^s$  and the transfer equation is simply

$$\frac{dI_\nu^s}{dl} = -\kappa_\nu I_\nu^s. \quad (3.2)$$

For the diffuse radiation we have

$$\frac{dI_\nu^d}{dl} = -\kappa_\nu I_\nu^d + j_\nu \quad (3.3)$$

together with boundary conditions which express the fact that there is no source of  $I_\nu^d$  outside the nebula.

3.1. *The diffuse radiation.*—About one third of all recombinations are on the  $n=1$  ground state and therefore the rate of production of quanta in the diffuse radiation field is about one third of the ionization rate. It follows that  $I_\nu^d$  is generally smaller than  $I_\nu^s$  and may be calculated by iterative methods.

For an optically thin nebula there is a small chance of a stellar quantum being absorbed and an even smaller chance that this is followed by emission, in the diffuse radiation field, of a quantum which is re-absorbed. In such a case a good first approximation would be to neglect the diffuse radiation. We concentrate our attention on another extreme, of nebulae for which the optical thickness is so large that no ionizing quanta escape.

If no diffuse radiation escapes,

$$\int \kappa_\nu J_\nu^d dV = \int j_\nu dV, \quad (3.4)$$

the integrals being over the entire nebular volume. In Approximation I we assume a similar relation for all points in the nebula.

$$\kappa_\nu J_\nu^d = j_\nu. \quad (\text{Approximation I}). \quad (3.5)$$

As Zanstra puts it, the diffuse radiation is re-absorbed “on the spot”.

For two reasons we expect Approximation I to give good results. The first is that, because we satisfy (3.4), we obtain correct results for the size of the ionized region. The second follows from the fact that we assume  $kT_e \ll h\nu_1$ . Then  $J_\nu^d = j_\nu / \kappa_\nu$ , given by (2.12), is large only for the lower frequencies,  $\nu$  close to  $\nu_1$ . At these frequencies,  $\kappa_\nu$  is large and a quantum will not travel far before it is absorbed.

As a check on Approximation I we may go to Approximation II, in which the transfer equation for  $I_\nu^d$  is solved using the values of  $j_\nu$  and  $\kappa_\nu$  obtained in Approximation I. This is done in § 8.

3.2. *The ionization equation and the thermal balance.*—The transfer equation in Approximation I is (3.2).

From  $\kappa_\nu J_\nu^d = j_\nu$  we have

$$4\pi \int \kappa_\nu J_\nu^d d\nu = 4\pi \int j_\nu d\nu = N_e N_+ \alpha_1 \quad (3.6)$$

and therefore, from (2.15)

$$4\pi \int \kappa_\nu J_\nu^s d\nu = N_e N_+ \alpha_B, \quad (\text{Approximation I}) \quad (3.7)$$

where

$$\alpha_B = \sum_{n=2}^{\infty} \alpha_n. \quad (3.8)$$

In a similar way we obtain from (2.17),

$$4\pi \int \kappa_\nu J_\nu^s h(\nu - \nu_1) d\nu = N_e N_+ kT_e \beta_B \quad (3.9)$$

where

$$\beta_B = \sum_{n=2}^{\infty} \beta_n + \beta_{ff}. \quad (3.10)$$

It is convenient to have analytic expressions for  $\alpha_B$  and  $\beta_B/\alpha_B$ . We find that the results of Seaton (1959, 1960) may be fitted to

$$\alpha_B = 1.627 \times 10^{-13} t_e^{-1/2} \{1 - 1.657 \log_{10} t_e + 0.584 t_e^{1/3}\}, \quad (3.11)$$

$$\beta_B/\alpha_B = 1.090 + 0.158 t_e \quad (3.12)$$

where  $t_e = 10^{-4} T_e$  ( $T_e$  in  $^{\circ}\text{K}$ ). For  $0.5 \leq t_e \leq 10$ , (3.11) gives  $\alpha_B$  to an accuracy of better than 1 per cent and for  $1 \leq t_e \leq 5$ , (3.12) gives  $\beta_B/\alpha_B$  with a similar accuracy.

4. *The plane-parallel case.*—We first solve (3.2), (3.7) and (3.9) for a plane parallel case. Later we show that the solutions may be adapted to the case of spherical symmetry.

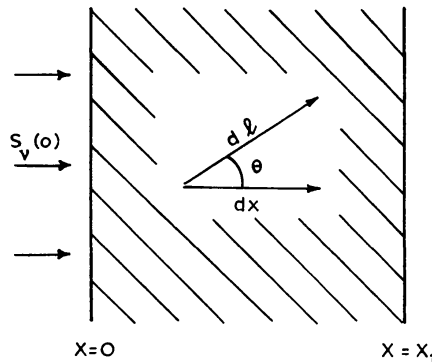


FIG. 1.—Geometry of plane-parallel models.

The geometry is shown in Fig. 1. In place of the photon intensity  $I_\nu^s$  we consider a photon flux  $S_\nu(x)$  per unit area:

$$I_\nu^s = \frac{\delta(1 - \cos \theta)}{2\pi} S_\nu, \quad (4.1)$$

where  $\delta(1 - \cos \theta)$  is a Dirac delta-function. For the mean intensity we have

$$4\pi J_\nu^s = S_\nu. \quad (4.2)$$

The equations of Approximation I become

$$\frac{d}{dx} S_\nu = -\kappa_\nu S_\nu, \quad (4.3)$$

$$\int_{\nu_1}^{\infty} \kappa_\nu S_\nu d\nu = N_e N_+ \alpha_B, \quad (4.4)$$

$$\int_{\nu_1}^{\infty} \kappa_\nu S_\nu h(\nu - \nu_1) d\nu = N_e N_+ kT_e \beta_B. \quad (4.5)$$

The flux at the inner boundary,  $S_\nu(0)$ , is a given function. The total number of ionizing quanta incident per  $\text{cm}^2$  per second is

$$\mathcal{Q} = \int_{\nu_1}^{\infty} S_\nu(0) d\nu. \quad (4.6)$$

We put

$$S_\nu(0) = \mathcal{Q} s_\nu(0), \quad (4.7)$$

where

$$\int_{\nu_1}^{\infty} s_\nu(0) d\nu = 1. \quad (4.8)$$

4.1. *Solutions in terms of the threshold optical depth.*—The method of de Jong (1951) depends on the fact that

$$\kappa_\nu = A N_H f_\nu,$$

is the product of a function of position times a function of frequency. We obtain solutions in terms of the threshold optical depth,

$$\tau = \int_0^x \kappa_{\nu_1} dx = A \int_0^x N_H dx. \quad (4.9)$$

Putting

$$S_\nu(\tau) = \mathcal{Q} s_\nu(\tau), \quad (4.10)$$

we have

$$s_\nu(\tau) = s_\nu(0) \exp(-\tau f_\nu). \quad (4.11)$$

We define

$$s(\tau) = \int_{\nu_1}^{\infty} s_\nu(\tau) d\nu, \quad (4.12)$$

$$u(\tau) = -\frac{d}{d\tau} s(\tau) = \int_{\nu_1}^{\infty} s_\nu(\tau) f_\nu d\nu, \quad (4.13)$$

$$w(\tau) = u^{-1}(\tau) \int_{\nu_1}^{\infty} s_\nu(\tau) f_\nu \left( \frac{\nu}{\nu_1} - 1 \right) d\nu. \quad (4.14)$$

The solution of the ionization equation is

$$A \mathcal{Q} N_H u(\tau) = N_e N_+ \alpha_B (T_e). \quad (4.15)$$

Dividing (4.5) by (4.4) we have, for the thermal balance,

$$w(\tau) = \left( \frac{kT_e}{h\nu_1} \right) \frac{\beta_B(T_e)}{\alpha_B(T_e)}. \quad (4.16)$$

Using the linear approximation, (3.11), for  $\beta_B/\alpha_B$ , we obtain  $T_e$  on solving a

quadratic equation, and with  $T_e(\tau)$  known, (4.15) gives  $N_H/N_e N_+$  as a function of  $\tau$ . Finally, the geometrical variable  $x$  is obtained from

$$x = A^{-1} \int_0^\tau N_H^{-1} d\tau. \quad (4.17)$$

4.2. *Models with constant ion density.*—If  $N_e = N_+$  is constant, we have

$$\frac{N_H}{N_+} = \frac{1}{2p(\tau)}, \quad (4.18)$$

where

$$p(\tau) = \frac{A\mathcal{Q}u(\tau)}{2N_+\alpha_B}. \quad (4.19)$$

The fraction of hydrogen which is neutral is

$$\xi = \frac{N_H}{N_+ + N_H} = \frac{1}{1 + 2p(\tau)}. \quad (4.20)$$

The geometrical variable is

$$x = \mathcal{Q} N_+^{-2} \int_0^\tau (u/\alpha_B) d\tau. \quad (4.21)$$

For isothermal models ( $T_e$  constant), these solutions become very simple. Since  $u = -ds/d\tau$  and  $s(0) = 1$  we obtain

$$x = x_1 (1 - s(\tau)), \quad (4.22)$$

where

$$x_1 = \mathcal{Q}/N_+^2 \alpha_B. \quad (4.23)$$

This has the following interpretation. As  $\tau \rightarrow \infty$ ,  $s(\tau) \rightarrow 0$  and  $x \rightarrow x_1$ . We may say that  $x_1$  is the length of the ionized column.  $\mathcal{Q}$ , the number of ionizing quanta incident per  $\text{cm}^2$ , is equal to  $N_+^2 \alpha_B x_1$ , the number of recombinations in the ionized column. Although  $N_+$  is constant, we may still speak of the gas as being neutral at  $x = x_1$ , since  $N_H$  goes to infinity and  $\xi$  goes to unity.

4.3. *Models with constant total hydrogen density.*—We have  $N_+ + N_H = N$ , where  $N$  is constant, and we put

$$N_H = \xi N, \quad N_+ = N_e = (1 - \xi) N. \quad (4.24)$$

From (4.15),

$$\frac{\xi}{(1 - \xi)^2} = \frac{1}{2p}, \quad (4.25)$$

where

$$p = \frac{A\mathcal{Q}u(\tau)}{2N\alpha_B}. \quad (4.26)$$

We obtain

$$\xi = (1 + p) - [(1 + p)^2 - 1]^{1/2} \quad (4.27)$$

and

$$x = (AN)^{-1} \int_0^\tau \xi^{-1} d\tau. \quad (4.28)$$

For isothermal models we define

$$x_1 = \mathcal{Q}/N^2 \alpha_B \quad (4.29)$$

and obtain

$$(1 - \xi)^2 / \xi = AN x_1 u(\tau) \quad (4.30)$$

or

$$\frac{1}{\xi} = AN x_1 u(\tau) + 2 - \xi. \quad (4.31)$$

Substitution in (4.28) gives

$$\frac{x}{x_1} = 1 - s(\tau) + (AN x_1)^{-1} \int_0^\tau (2 - \xi) d\tau, \quad (4.32)$$

which is a convenient form for numerical integration.

For  $p \gg 1$ , (4.27) is most easily evaluated using the expansion

$$\xi = \frac{1}{2q} \left[ 1 + \frac{1}{4q^2} + \frac{1}{8q^4} + \dots \right] \quad (4.33)$$

where  $q = 1 + p$ .

5. *Spherically symmetric models.*—In these models the mean intensity of ionizing radiation is determined by an attenuation factor,  $\exp(-\tau f_\nu)$ , and a geometrical dilution factor,  $(r_s/r)^2$ , and it is therefore more difficult to separate the optical and the geometrical variables. For the case of isothermal models with constant total hydrogen density it is no longer possible to express the solution in terms of quadratures, as in §4.2, but we shall show that solutions may be obtained using a rapidly converging iterative procedure.

5.1. *General formulation.*—We consider a sphere of radius  $r$  with the star at its centre. Let  $L_\nu(r)$  be the number of stellar quanta crossing this sphere per unit time. Then

$$L_\nu = 4\pi r^2 S_\nu \quad (5.1)$$

where  $S_\nu$  is the flux per unit area. The equations of radiative transfer and of ionization equilibrium become

$$\frac{d}{dr} L_\nu = -\kappa_\nu L_\nu \quad (5.2)$$

$$\int \kappa_\nu L_\nu d\nu = 4\pi r^2 \alpha_B N_e N_+. \quad (5.3)$$

Suppose that the inner boundary of the ionized region is at  $r = r_0$  ( $N = N_+ + N_H = 0$  for  $r < r_0$ ) and define the optical depth

$$\tau = \int_{r_0}^r AN_H dr. \quad (5.4)$$

Put

$$L_\nu(r_0) = \mathcal{N} s_\nu(0), \quad (5.5)$$

where

$$\int_{\nu_1}^{\infty} s_\nu(0) d\nu = 1.$$

Then  $\mathcal{N}$  is the total number of ionizing quanta emitted by the star per second. The solution of the transfer equation is

$$L_\nu(r) = \mathcal{N} s_\nu(\tau), \quad (5.6)$$

where

$$s_\nu(\tau) = s_\nu(0) \exp(-\tau f_\nu) \quad (5.7)$$

as in §4.1. The solution of the ionization equation is

$$\frac{N_H}{N_e N_+} = \frac{4\pi r^2 \alpha_B}{A \mathcal{N} u(\tau)}. \quad (5.8)$$

5.2. *Isothermal models with constant ion density.*—We have

$$A N_H dr = d\tau \quad (5.9)$$

and using (5.8),

$$\frac{4\pi \alpha_B N_+^2}{3 \mathcal{N}} dr^3 = u d\tau. \quad (5.10)$$

With  $N_+$  constant and  $\alpha_B$  constant this may be integrated to give

$$\frac{4\pi \alpha_B N_+^2}{3 \mathcal{N}} (r^3 - r_0^3) = 1 - s(\tau). \quad (5.11)$$

For  $\tau \rightarrow \infty$  we have  $s(\tau) \rightarrow 0$  and  $r \rightarrow r_1$ , where

$$\mathcal{N} = \frac{4\pi}{3} \alpha_B N_+^2 (r_1^3 - r_0^3). \quad (5.12)$$

Then  $r_1$  is the radius of the ionized region and (5.12) expresses the fact that the number of ionizing quanta is equal to the number of recombinations in the ionized volume. Defining

$$\rho = \frac{r}{r_1}, \quad \rho_0 = \frac{r_0}{r_1}, \quad (5.13)$$

we have

$$1 - \rho^3 = (1 - \rho_0^3) s(\tau). \quad (5.14)$$

The ionization equation becomes

$$r_1 A N_H = \frac{3\rho^2}{(1 - \rho_0^3) u(\tau)} \quad (5.15)$$

and

$$\xi = \frac{N_H}{N_+ + N_H} = \frac{1}{1 + 2p}, \quad (5.16)$$

where

$$p = A N_+ r_1 (1 - \rho_0^3) u(\tau) / 6\rho^2. \quad (5.17)$$

5.3. *Isothermal models with constant total hydrogen density.*—With  $\alpha_B$  constant and  $N_H = \xi N$ ,  $N_+ = N_e = (1 - \xi)N$ , where  $N$  is constant, we define  $r_1$  by

$$\mathcal{N} = \frac{4\pi}{3} \alpha_B N^2 (r_1^3 - r_0^3). \quad (5.18)$$

The ionization equation is then

$$\frac{(1 - \xi)^2}{\xi} = \frac{A N r_1 (1 - \rho_0^3) u(\tau)}{3\rho^2}, \quad (5.19)$$

giving

$$\xi = 1 + p - [(1 + p)^2 - 1]^{1/2}, \quad (5.20)$$

where

$$p = \frac{ANr_1(1-\rho_0^3)u(\tau)}{6\rho^2}. \quad (5.21)$$

From (5.8) and (5.9) we have

$$\frac{4\pi\alpha_B N^2 dr^3}{3\mathcal{N}} = \frac{u(\tau) d\tau}{(1-\xi)^2} \quad (5.22)$$

and integration gives

$$\frac{\rho^3 - \rho_0^3}{1 - \rho_0^3} = \int_0^\tau \frac{u(\tau) d\tau}{(1-\xi)^2}. \quad (5.23)$$

From (5.19) we have

$$\frac{u(\tau)}{(1-\xi)^2} = u(\tau) + \frac{3\rho^2(2-\xi)}{ANr_1(1-\rho_0^3)}. \quad (5.24)$$

Using  $\int_0^\tau u(\tau) d\tau = 1 - s$  we obtain

$$1 - \rho^3 = (1 - \rho_0^3)s(\tau) - 3(ANr_1)^{-1} \int_0^\tau \rho^2(2-\xi) d\tau. \quad (5.25)$$

The equations (5.20) and (5.25) may be solved by iteration. We neglect the integral in (5.25) to obtain  $1 - \rho^3 = (1 - \rho_0^3)s(\tau)$  giving a first approximation to  $\rho(\tau)$ . From (5.20), (5.21) we then obtain a first approximation to  $\xi(\tau)$ . With these results we may calculate the integral  $\int \rho^2(2-\xi) d\tau$  and hence obtain a second approximation in  $\rho$  and  $\xi$ . In practice this procedure converges very rapidly.

6. *Black body radiation.*—We consider that the star radiates as a black body at temperature  $T_s$ . At the surface of the star the flux is  $\pi\mathcal{B}_\nu(T_s)$  photons  $\text{cm}^{-2} \text{sec}^{-1}$  where  $\mathcal{B}_\nu$  is given by (2.14). The function  $s_\nu(0)$  defined by (4.7), (4.8) is

$$s_\nu(0) = \frac{h}{kT_s} \cdot \frac{v^2[\exp(v) - 1]^{-1}}{F(T_s)}, \quad (6.1)$$

where

$$v = h\nu/kT_s, \quad v_1 = h\nu_1/kT_s \quad (6.2)$$

and

$$F(T_s) = \int_{\alpha_1}^{\infty} v^2 [\exp(v) - 1]^{-1} dv. \quad (6.3)$$

TABLE I

$10^{-4} T_s$	$F(T_s)$
1	3.9311 - 5
2	2.9870 - 2
3	2.0881 - 1
4	4.9565 - 1
5	7.9021 - 1
6	1.0483
8	1.4345
10	1.6876
12	1.8569
15	2.0192
20	2.1665

TABLE II

$10^{-4} T_s$	$s(\tau)$				
	1	2	3	4	5
$\tau$					
0.0	1.000	1.000	1.000	1.000	1.000
0.1	9.189-1	9.306-1	9.404-1	9.484-1	9.551-1
0.2	8.445-1	8.664-1	8.848-1	9.001-1	9.128-1
0.3	7.762-1	8.070-1	8.330-1	8.548-1	8.729-1
0.5	6.562-1	7.008-1	7.395-1	7.724-1	8.001-1
0.7	5.551-1	6.096-1	6.581-1	6.998-1	7.352-1
1.0	4.324-1	4.962-1	5.547-1	6.063-1	6.509-1
1.5	2.862-1	3.550-1	4.220-1	4.834-1	5.378-1
2.0	1.904-1	2.569-1	3.256-1	3.911-1	4.509-1
2.5	1.273-1	1.880-1	2.547-1	3.209-1	3.830-1
3.0	8.560-2	1.391-1	2.019-1	2.668-1	3.292-1
4.0	3.939-2	7.891-2	1.317-1	1.908-1	2.508-1
5.0	1.860-2	4.683-2	8.988-2	1.419-1	1.975-1
7.0	4.519-3	1.867-2	4.665-2	8.587-2	1.320-1
10.0	6.831-4	6.029-3	2.116-2	4.699-2	8.130-2
15.0	5.232-5	1.408-3	7.677-3	2.164-2	4.352-2
20.0	6.819-6	4.496-4	3.456-3	1.172-2	2.652-2
30.0	2.901-7	7.628-5	9.941-4	4.488-3	1.217-2
50.0	3.241-9	6.024-6	1.657-4	1.122-3	3.932-3
70.0		9.228-7	4.385-5	3.993-4	1.690-3
100.0		1.040-7	9.294-6	1.193-4	6.278-4
150.0		6.669-9	1.312-6	2.585-5	1.787-4
200.0			2.856-7	7.835-6	6.690-5
250.0			8.053-8	2.904-6	2.951-5
300.0			2.704-8	1.233-6	1.455-5
400.0				2.921-7	4.427-6
500.0				8.839-8	1.647-6
700.0					3.299-7
1000.0					5.092-8

For the integrals of § 4.1 we have

$$s(\tau) = F^{-1}(T_s) \int_{\alpha_1}^{\infty} v^2 [\exp(v) - 1]^{-1} \exp[-\tau f(v/v_1)] dv, \quad (6.4)$$

$$u(\tau) = F^{-1}(T_s) \int_{\alpha_1}^{\infty} v^2 [\exp(v) - 1]^{-1} \exp[-\tau f(v/v_1)] f(v/v_1) dv, \quad (6.5)$$

$$w(\tau) = [u(\tau) F(T_s)]^{-1} \int_{\alpha_1}^{\infty} v^2 [\exp(v) - 1]^{-1} \exp[-\tau f(v/v_1)] f(v/v_1) (v/v_1 - 1) dv. \quad (6.6)$$

For numerical calculation we use

$$hv_1/k = 157890 \text{ }^\circ\text{K.}$$

The functions  $F$ ,  $s$ ,  $u$ , and  $w$  are given in Tables I to IV. The integrals were evaluated on the University of London Mercury Computer, using the 24- and 32-point Gauss-Laguerre formulae given by Rabinowitz and Weiss (1959). The results are thought to be accurate to within two digits in the last figure.

TABLE II (continued)

$10^{-4} T_s$	6	8	10	12	15	20
$\tau$						
0.0	1.000	1.000	1.000	1.000	1.000	1.000
0.1	9.605-1	9.689-1	9.748-1	9.792-1	9.839-1	9.888-1
0.2	9.232-1	9.393-1	9.508-1	9.594-1	9.685-1	9.780-1
0.3	8.880-1	9.113-1	9.280-1	9.404-1	9.537-1	9.677-1
0.5	8.232-1	8.593-1	8.854-1	9.049-1	9.259-1	9.481-1
0.7	7.652-1	8.122-1	8.466-1	8.723-1	9.003-1	9.299-1
1.0	6.890-1	7.496-1	7.944-1	8.283-1	8.653-1	9.049-1
1.5	5.854-1	6.625-1	7.208-1	7.654-1	8.148-1	8.682-1
2.0	5.041-1	5.923-1	6.602-1	7.130-1	7.720-1	8.367-1
2.5	4.394-1	5.347-1	6.096-1	6.685-1	7.352-1	8.091-1
3.0	3.871-1	4.868-1	5.666-1	6.303-1	7.030-1	7.846-1
4.0	3.085-1	4.119-1	4.976-1	5.676-1	6.493-1	7.429-1
5.0	2.530-1	3.561-1	4.444-1	5.181-1	6.058-1	7.081-1
7.0	1.810-1	2.785-1	3.670-1	4.439-1	5.383-1	6.513-1
10.0	1.211-1	2.070-1	2.911-1	3.678-1	4.660-1	5.898-1
15.0	7.191-2	1.406-1	2.149-1	2.872-1	3.851-1	5.156-1
20.0	4.752-2	1.032-1	1.684-1	2.353-1	3.299-1	4.621-1
30.0	2.473-2	6.326-2	1.143-1	1.711-1	2.574-1	3.870-1
50.0	9.553-3	3.086-2	6.450-2	1.067-1	1.778-1	2.966-1
70.0	4.683-3	1.797-2	4.183-2	7.455-2	1.340-1	2.416-1
100.0	2.025-3	9.483-3	2.503-2	4.865-2	9.559-2	1.887-1
150.0	6.974-4	4.193-3	1.296-2	2.809-2	6.176-2	1.370-1
200.0	3.024-4	2.206-3	7.706-3	1.818-2	4.364-2	1.060-1
250.0	1.507-4	1.290-3	4.985-3	1.262-2	3.258-2	8.530-2
300.0	8.247-5	8.099-4	3.416-3	9.185-3	2.525-2	7.057-2
400.0	2.988-5	3.693-4	1.802-3	5.362-3	1.638-2	5.108-2
500.0	1.284-5	1.918-4	1.056-3	3.417-3	1.139-2	3.890-2
700.0	3.246-6	6.591-5	4.408-4	1.634-3	6.269-3	2.483-2
1000.0	6.552-7	1.895-5	1.587-4	6.878-4	3.108-3	1.461-2
1500.0	8.753-8	3.935-6	4.362-5	2.298-4	1.274-3	7.420-3
2000.0		1.157-6	1.592-5	9.758-5	6.330-4	4.354-3
2500.0		4.190-7	6.892-6	4.783-5	3.534-4	2.788-3
3000.0			3.346-6	2.584-5	2.134-4	1.894-3
4000.0			9.940-7	9.174-6	9.131-5	9.867-4
5000.0			3.630-7	3.881-6	4.505-5	5.727-4

## 7. Illustrative calculations

7.1. *Plane parallel models.*—Let the inner boundary of a nebula be at a distance  $r_0$  from a star of radius  $r_s$ , which radiates as a black body at temperature  $T_s$ . Then

$$S_\nu(r_0) = \left(\frac{r_s}{r_0}\right)^2 \pi \mathcal{B}_\nu(T_s)$$

and

$$\mathcal{Q} = \frac{2\pi}{c^2} \left(\frac{kT_s}{h}\right)^3 \left(\frac{r_s}{r_0}\right)^2 F(T_s).$$

With  $r_0 = 10^6 r_s$ ,  $T_s = 4 \times 10^4$  K, this gives  $\mathcal{Q} = 2.00 \times 10^{12}$  photons  $\text{cm}^{-2} \text{sec}^{-1}$ . We consider plane parallel models with this value of  $\mathcal{Q}$ .

(i) *A model with constant total hydrogen density and variable temperature.*—We take

$$N = N_+ + N_H = 10^4 \text{ cm}^{-3}.$$

TABLE III

$10^{-4} T_e$	$u(\tau)$				
	1	2	3	4	5
$\tau$					
0.0	8.468-1	7.208-1	6.174-1	5.328-1	4.634-1
0.1	7.766-1	6.672-1	5.754-1	4.991-1	4.359-1
0.2	7.124-1	6.178-1	5.365-1	4.678-1	4.103-1
0.3	6.535-1	5.722-1	5.004-1	4.387-1	3.864-1
0.5	5.502-1	4.913-1	4.359-1	3.864-1	3.433-1
0.7	4.635-1	4.224-1	3.804-1	3.411-1	3.058-1
1.0	3.588-1	3.375-1	3.112-1	2.841-1	2.582-1
1.5	2.348-1	2.338-1	2.248-1	2.117-1	1.972-1
2.0	1.543-1	1.634-1	1.643-1	1.601-1	1.529-1
2.5	1.018-1	1.153-1	1.217-1	1.227-1	1.203-1
3.0	6.747-2	8.210-2	9.118-2	9.537-2	9.605-2
4.0	3.008-2	4.294-2	5.318-2	5.996-2	6.371-2
5.0	1.370-2	2.342-2	3.255-2	3.958-2	4.432-2
7.0	3.059-3	7.885-3	1.388-2	1.950-2	2.405-2
10.0	3.982-4	2.032-3	4.969-3	8.421-3	1.172-2
15.0	2.369-5	3.571-4	1.360-3	2.938-5	4.772-3
20.0	2.513-6	9.287-5	5.001-4	1.305-3	2.389-3
30.0	7.944-8	1.177-5	1.079-4	3.763-4	8.291-4
50.0	6.096-10	6.416-7	1.249-5	6.556-5	1.876-4
70.0		7.690-8	2.593-6	1.837-5	6.363-5
100.0		6.673-9	4.244-7	4.248-6	1.835-5
150.0		3.176-10	4.460-8	6.871-7	3.908-6
200.0			7.865-9	1.690-7	1.189-6
250.0			1.882-9	5.325-8	4.465-7
300.0			5.526-10	1.979-8	1.929-7
400.0				3.798-9	4.759-8
500.0				9.753-10	1.504-8
700.0					2.354-9
1000.0					2.795-10

We calculate  $T_e(\tau)$  from (4.16),  $\xi(\tau)$  from (4.27) and  $x(\tau)$  from (4.28). Figure 2 shows: (a)  $T_e(\tau)$ , (b)  $x(\tau)$  and (c)  $\log \xi$  as a function of  $x$ .

For large  $\tau$  the quanta close to the Lyman limit have all been absorbed and the ionization which still occurs is produced by quanta of higher energy. The photoelectrons produced have large kinetic energies and in consequence  $T_e$  becomes large. In real nebulae  $T_e$  is much reduced by electron excitation of ions such as  $O^+$ ,  $N^+$  and  $O^{+2}$ , but even for a pure hydrogen nebula the high temperatures we obtain are unrealistic. Except for the smallest values of  $\tau$ , we obtain values of  $T_e$  which do not satisfy the inequality  $kT_e \ll h\nu_1$  and when this is violated collisional excitation and ionization of hydrogen can no longer be neglected.

We shall return to the problem of the energy balance in later papers of this series. In the remainder of the present paper we shall treat only isothermal models and in practice we adopt  $T_e = 1 \times 10^4$  °K.

(ii) *Isothermal models.*—Fig. 2 (d) shows  $\log \xi$  against  $x$  for a model which is isothermal,  $T_e = 1 \times 10^4$  °K, but otherwise the same as the model of §7.1.1. At the lower electron temperature the recombination coefficient is larger and the size of the ionized region is much reduced.

TABLE III (continued)

$10^{-4} T_s$	6	8	10	12	15	20
$\tau$						
0.0	4.064-1	3.197-1	2.581-1	2.130-1	1.646-1	1.144-1
0.1	3.836-1	3.032-1	2.457-1	2.032-1	1.576-1	1.099-1
0.2	3.622-1	2.878-1	2.340-1	1.940-1	1.510-1	1.057-1
0.3	3.423-1	2.734-1	2.231-1	1.855-1	1.448-1	1.017-1
0.5	3.063-1	2.472-1	2.032-1	1.699-1	1.334-1	9.431-2
0.7	2.748-1	2.241-1	1.856-1	1.561-1	1.233-1	8.777-2
1.0	2.346-1	1.945-1	1.629-1	1.382-1	1.102-1	7.923-2
1.5	1.826-1	1.557-1	1.330-1	1.144-1	9.262-2	6.775-2
2.0	1.444-1	1.266-1	1.103-1	9.624-2	7.914-2	5.885-2
2.5	1.159-1	1.046-1	9.293-2	8.220-2	6.860-2	5.183-2
3.0	9.443-2	8.769-2	7.937-2	7.116-2	6.024-2	4.621-2
4.0	6.519-2	6.396-2	6.002-2	5.519-2	4.798-2	3.785-2
5.0	4.711-2	4.867-2	4.721-2	4.443-2	3.957-2	3.200-2
7.0	2.738-2	3.098-2	3.183-2	3.118-2	2.892-2	2.441-2
10.0	1.452-2	1.835-2	2.021-2	2.076-2	2.023-2	1.796-2
15.0	6.584-3	9.582-3	1.153-2	1.258-2	1.305-2	1.236-2
20.0	3.585-3	5.821-3	7.503-3	8.589-3	9.355-3	9.317-3
30.0	1.415-3	2.723-3	3.905-3	4.812-3	5.655-3	6.095-3
50.0	3.845-4	9.406-4	1.570-3	2.150-3	2.817-3	3.397-3
70.0	1.491-4	4.349-4	8.120-4	1.201-3	1.705-3	2.237-3
100.0	5.015-5	1.794-4	3.812-4	6.169-4	9.617-4	1.390-3
150.0	1.296-5	5.976-5	1.493-4	2.705-4	4.740-4	7.745-4
200.0	4.574-6	2.568-5	7.270-5	1.437-4	2.759-4	4.961-4
250.0	1.942-6	1.282-5	4.024-5	8.548-5	1.770-4	3.442-4
300.0	9.320-7	7.072-6	2.426-5	5.483-5	1.211-4	2.520-4
400.0	2.742-7	2.625-6	1.044-5	2.618-5	6.440-5	1.503-4
500.0	1.002-7	1.162-6	5.223-6	1.426-5	3.837-5	9.842-5
700.0	1.982-8	3.131-7	1.715-6	5.374-6	1.670-5	4.987-5
1000.0	3.081-9	6.951-8	4.777-7	1.755-6	6.442-6	2.295-5
1500.0	3.055-10	1.074-8	9.790-8	4.383-7	1.979-6	8.779-6
2000.0		2.557-9	2.899-8	1.512-7	8.010-7	4.209-6
2500.0		7.858-10	1.066-8	6.303-8	3.810-7	2.302-6
3000.0			4.529-9	2.982-8	2.018-7	1.374-6
4000.0			1.089-9	8.580-9	7.009-8	5.826-7
5000.0			3.375-10	3.083-9	2.940-8	2.882-7

With  $T_e = 1 \times 10^4$  °K we have  $\alpha_B = 2.58 \times 10^{-13} \text{ cm}^{-3} \text{ sec}^{-1}$  and, with  $\mathcal{Q} = 2.00 \times 10^{12}$ ,  $N = 10^4$ , this gives  $x_1 = 0.778 \times 10^{17} \text{ cm}$ . Fig. 3 shows the structure of the transition region,  $x/x_1$  close to unity, for models with black body radiation,  $T_s = 4 \times 10^4$  °K. Curve (a) is for a model with constant ion density  $N_+ = 10^4 \text{ cm}^{-3}$  and curve (b), for constant total hydrogen density,  $N = N_+ + N_H = 10^4 \text{ cm}^{-3}$ . Curve (a) is the case considered by de Jong (1951).

With constant ion density,  $\xi$  rises to unity at  $x = x_1$ . For  $x$  much less than  $x_1$ ,  $\xi$  is small for the models with constant total hydrogen density and  $N_+$  is then sensibly constant. In consequence, curves (a) and (b) coincide for small  $x/x_1$ . The transition region for constant total hydrogen density is obviously less sharp than that for constant ion density.

The structure of the transition region depends on the frequency distribution of the ionizing radiation. Quanta of high frequency have a small absorption coefficient and are able to penetrate further; thus the tail of the ionized region is

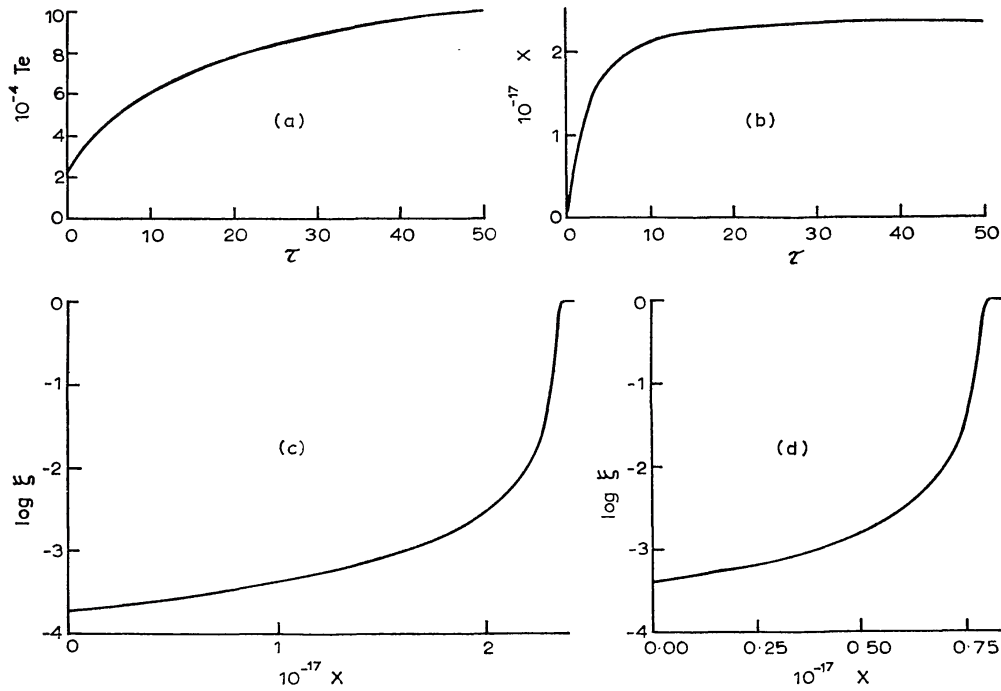


FIG. 2.—Results of a plane parallel model with  $\mathcal{Q} = 2.00 \times 10^{12}$  photons  $\text{cm}^{-1} \text{sec}^{-1}$ ,  $T_s = 4 \times 10^4 \text{K}$  and  $N = 10^4 \text{cm}^{-3}$ . Curve (a) gives the relation between  $T_e$  and  $\tau$  obtained from (4.16); (b) and (c) give the resulting relations between  $x$  and  $\tau$  and between  $\log \xi$  and  $x$ ; (d) gives the relation between  $\log \xi$  and  $x$  for an isothermal model with  $T_e = 1 \times 10^4 \text{K}$ .

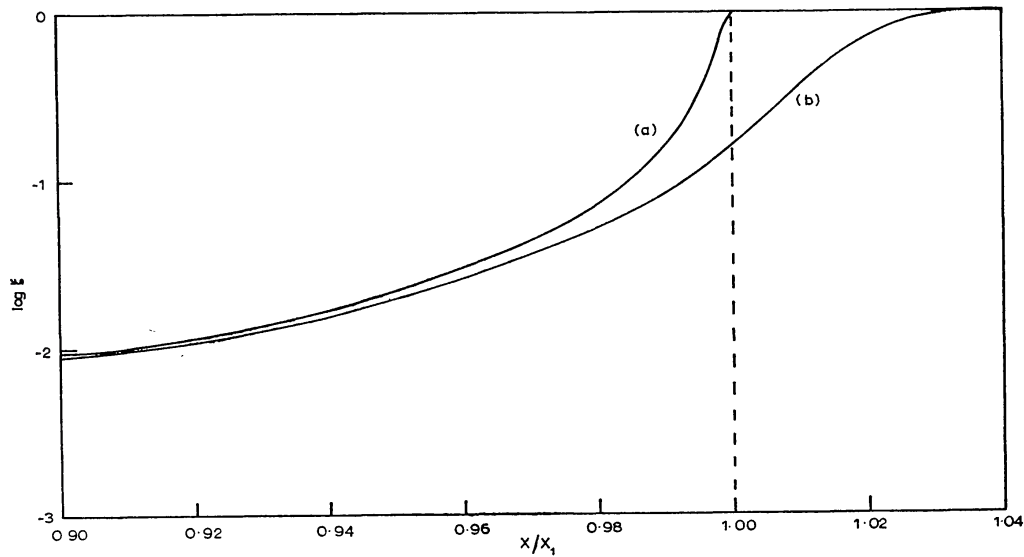


FIG. 3.—The transition region for isothermal plane parallel models with black body radiation,  $T_s = 4 \times 10^4 \text{K}$ ,  $\mathcal{Q} = 2.00 \times 10^{12}$  photons  $\text{cm}^{-1} \text{sec}^{-1}$ ,  $T_e = 10^4 \text{K}$ :

(a) Constant ion density,  $N_+ = 10^4 \text{cm}^{-3}$ ,

(b) Constant total hydrogen density,  $N = N_+ + N_H = 10^4 \text{cm}^{-3}$ .

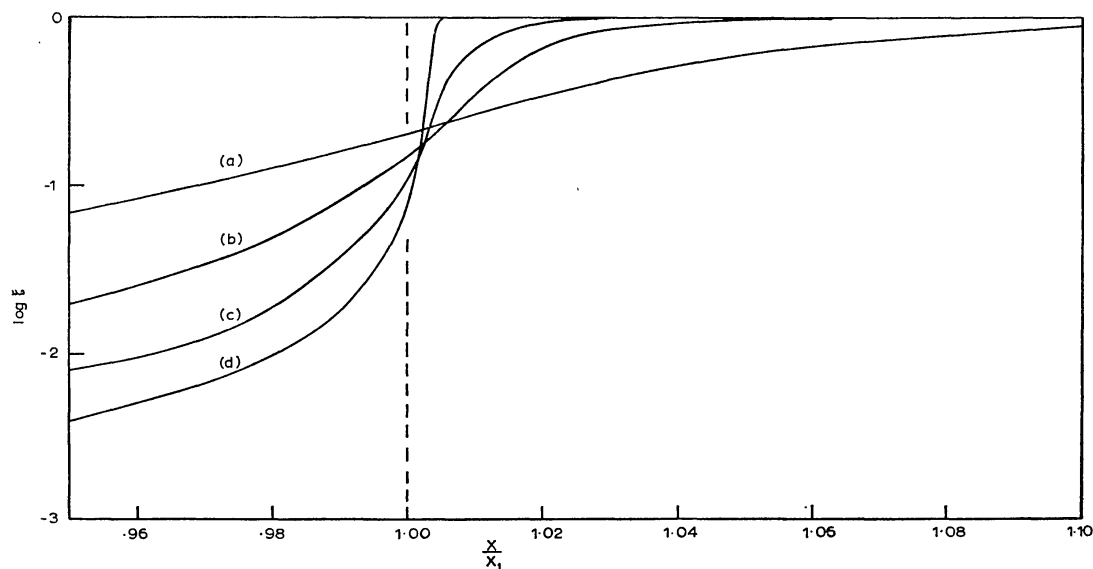


FIG. 4.—The transition region for isothermal plane parallel models with black body radiation with constant stellar flux,  $\mathcal{Q} = 2.00 \times 10^{12}$  photons  $\text{cm}^{-1} \text{sec}^{-1}$ ,  $T_e = 10^4$  °K:

- (a)  $T_g = 8 \times 10^4$  °K,
- (b)  $T_g = 4 \times 10^4$  °K,
- (c)  $T_g = 2 \times 10^4$  °K,
- (d) monochromatic radiation,  $\nu = \nu_1$ .

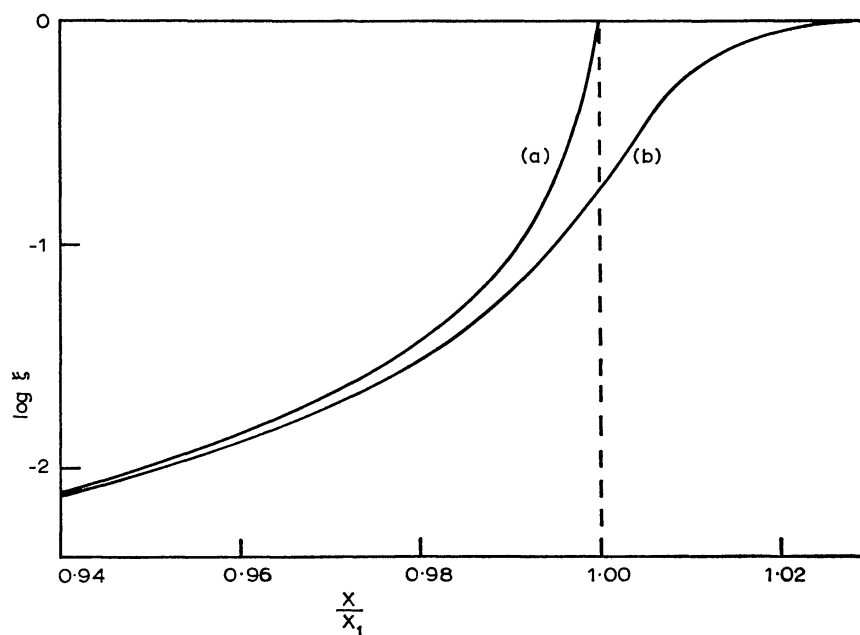


FIG. 5.—The transition region for the spherically symmetric models of § 7.2.

- (a) Constant ion density,  $N_+ = 10^4 \text{ cm}^{-3}$ .
- (b) Constant total hydrogen density,  $N = 10^4 \text{ cm}^{-3}$ .

TABLE IV

$10^{-4} T_s$	$w(\tau)$				
	1	2	3	4	5
$\tau$					
0.0	6.093-2	1.179-1	1.715-1	2.218-1	2.691-1
0.1	6.162-2	1.198-1	1.748-1	2.266-1	2.751-1
0.2	6.232-2	1.219-1	1.783-1	2.315-1	2.813-1
0.3	6.303-2	1.239-1	1.818-1	2.364-1	2.876-1
0.5	6.450-2	1.281-1	1.890-1	2.465-1	3.004-1
0.7	6.600-2	1.325-1	1.965-1	2.570-1	3.136-1
1.0	6.836-2	1.394-1	2.082-1	2.732-1	3.339-1
1.5	7.255-2	1.517-1	2.289-1	3.016-1	3.692-1
2.0	7.708-2	1.650-1	2.510-1	3.315-1	4.059-1
2.5	8.199-2	1.793-1	2.744-1	3.626-1	4.433-1
3.0	8.729-2	1.947-1	2.988-1	3.944-1	4.812-1
4.0	9.917-2	2.281-1	3.501-1	4.591-1	5.563-1
5.0	1.129-1	2.645-1	4.028-1	5.230-1	6.285-1
7.0	1.459-1	3.421-1	5.059-1	6.420-1	7.589-1
10.0	2.080-1	4.565-1	6.424-1	7.922-1	9.195-1
15.0	3.235-1	6.160-1	8.211-1	9.846-1	1.123
20.0	4.273-1	7.416-1	9.599-1	1.134	1.281
30.0	5.900-1	9.348-1	1.173	1.363	1.523
50.0	8.200-1	1.208	1.474	1.686	1.864
70.0		1.407	1.695	1.922	2.113
100.0		1.637	1.949	2.194	2.400
150.0		1.925	2.266	2.534	2.759
200.0			2.510	2.796	3.036
250.0			2.712	3.013	3.264
300.0			2.886	3.199	3.460
400.0				3.509	3.788
500.0				3.765	4.058
700.0					4.493
1000.0					4.995

determined by the tail of the photon distribution. This is illustrated in Fig. 4, which shows the transition region for a series of isothermal models,  $T_e = 1 \times 10^4$  °K with constant incident flux,  $\mathcal{Q} = 2.00 \times 10^{12}$  photons  $\text{cm}^{-1} \text{sec}^{-1}$ . Curves (a), (b), (c) and (d) correspond to black body flux distribution with  $T_s = 8, 4, 2,$  and  $0 \times 10^4$  °K; curve (d) is the case of monochromatic radiation of frequency  $\nu_1$ , previously considered by Strömgren (1939). Monochromatic radiation of frequency  $\nu_1$  has a large absorption coefficient and curve (d) therefore shows a very sharp transition region.

7.2. *Spherically symmetric models.*—Calculations have been made for models with  $T_s = 4 \times 10^4$  °K,  $r_s = R_\odot = 6.96 \times 10^{10}$  cm,  $r_0 = 0$ ,  $T_e = 1 \times 10^4$  °K. Model (a) has constant ion density,  $N_+ = 10^4 \text{ cm}^{-3}$ . Equation (5.18) may be written

$$\frac{8\pi^2 r_s^2}{c^2} \left( \frac{kT_s}{h} \right)^3 F(T_s) = \frac{4\pi}{3} \alpha_B N^2 (r_1^3 - r_0^3).$$

This gives  $r_1 = 1.042 \times 10^{17}$  cm. Model (b) has constant total hydrogen density  $N = 1 \times 10^4 \text{ cm}^{-3}$ . The value of  $r_1$  is as for model (a).

TABLE IV (continued)

$10^{-4} T_s$	6	8	10	12	15	20
$\tau$						
0.0	3.133-1	3.939-1	4.656-1	5.302-1	6.164-1	7.390-1
0.1	3.206-1	4.034-1	4.770-1	5.432-1	6.316-1	7.572-1
0.2	3.280-1	4.130-1	4.885-1	5.563-1	6.469-1	7.754-1
0.3	3.355-1	4.227-1	5.000-1	5.696-1	6.623-1	7.937-1
0.5	3.508-1	4.424-1	5.235-1	5.962-1	6.931-1	8.302-1
0.7	3.665-1	4.624-1	5.472-1	6.231-1	7.241-1	8.667-1
1.0	3.906-1	4.929-1	5.831-1	6.637-1	7.705-1	9.211-1
1.5	4.320-1	5.446-1	6.433-1	7.311-1	8.471-1	1.010
2.0	4.744-1	5.968-1	7.033-1	7.967-1	9.217-1	1.095
2.5	5.174-1	6.485-1	7.620-1	8.621-1	9.935-1	1.177
3.0	5.602-1	6.992-1	8.189-1	9.242-1	1.062	1.254
4.0	6.437-1	7.960-1	9.259-1	1.040	1.188	1.394
5.0	7.225-1	8.849-1	1.023	1.143	1.300	1.517
7.0	8.620-1	1.039	1.188	1.318	1.488	1.722
10.0	1.031	1.222	1.384	1.525	1.708	1.962
15.0	1.245	1.453	1.629	1.782	1.982	2.260
20.0	1.410	1.630	1.817	1.980	2.193	2.489
30.0	1.663	1.903	2.106	2.283	2.515	2.838
50.0	2.019	2.286	2.511	2.709	2.967	3.329
70.0	2.280	2.566	2.807	3.019	3.296	3.682
100.0	2.580	2.888	3.148	3.375	3.673	4.091
150.0	2.955	3.290	3.572	3.819	4.143	4.598
200.0	3.244	3.600	3.899	4.161	4.505	4.986
250.0	3.483	3.855	4.169	4.444	4.802	5.307
300.0	3.688	4.074	4.400	4.685	5.058	5.583
400.0	4.030	4.441	4.787	5.089	5.485	6.041
500.0	4.312	4.743	5.105	5.422	5.836	6.416
700.0	4.767	5.230	5.619	5.958	6.402	7.025
1000.0	5.291	5.791	6.210	6.576	7.053	7.722
1500.0	5.943	6.490	6.947	7.344	7.864	8.591
2000.0		7.028	7.514	7.937	8.488	9.260
2500.0		7.471	7.982	8.424	9.001	9.808
3000.0			8.382	8.843	9.443	1.028 + I
4000.0			9.051	9.541	1.018 + I	1.107 + I
5000.0			9.601	1.012 + I	1.078 + I	1.171 + I

For model (a) our equations are

$$\rho^3 = 1 - s(\tau),$$

$$p(\tau) = \frac{6565 u(\tau)}{6\rho^2},$$

$$\xi = \frac{1}{1 + 2p},$$

where  $\rho = r/r_1$ , and for model (b) they are

$$\rho^3 = 1 - s(\tau) + \frac{3}{6565} \int_0^\tau \rho^2 (2 - \xi) d\tau,$$

$$p(\tau) = \frac{6565 u(\tau)}{6\rho^2},$$

$$\xi = 1 + p - [(1 + p)^2 - 1]^{1/2}.$$

These equations are readily solved by the iteration procedure described in § 5.3, in which one starts with the approximation  $\rho^3 = 1 - s(\tau)$ . The second iteration gives accurate solutions.

Fig. 5 shows the results obtained for the structure of the transition region.

8. *Approximation II for plane parallel isothermal models.*—For the diffuse radiation the transfer equation is

$$\frac{\mu}{f_\nu} \frac{d}{d\tau} I_\nu^d(\tau, \mu) = -I_\nu^d(\tau, \mu) + \mathcal{S}_\nu(\tau), \quad (8.1)$$

where  $\mu = \cos \theta$  and

$$\mathcal{S}_\nu = \frac{j_\nu}{\kappa_\nu} = \frac{N_e N_+}{N_H} \left( \frac{h^2}{2\pi m k T_e} \right)^{3/2} 2 \left( \frac{\nu}{c} \right)^2 \exp [h(\nu_1 - \nu)/kT_e]. \quad (8.2)$$

We take the inner boundary condition to be

$$I_\nu^d(0, \mu) = I_\nu^d(0, -\mu), \quad (8.3)$$

which is the same as the condition at the inner boundary of a spherically symmetric nebula. With  $\tau = \tau_e$  at the outer boundary, we have

$$I_\nu^d(\tau_e, \mu) = 0, \quad \mu < 0, \quad (8.4)$$

since there is no incident diffuse radiation. The solution of (8.1) is then

$$I_\nu^d(\tau, \mu) = \exp(-f_\nu \tau / \mu) \left\{ \int_0^\tau \exp(f_\nu \tau' / \mu) \mathcal{S}_\nu(\tau') \frac{f_\nu}{\mu} d\tau' + \int_0^{\tau_e} \exp(-f_\nu \tau' / |\mu|) \mathcal{S}_\nu(\tau') \frac{f_\nu}{|\mu|} d\tau' \right\}. \quad (8.5)$$

In Approximation I we put

$$J_\nu^d = \mathcal{S}_\nu^I \quad (\text{Approximation I}) \quad (8.6)$$

and obtain (§ 4.1)

$$\frac{N_e N_+}{N_H} = \frac{A \mathcal{Q} u(\tau)}{\alpha_B(T_e)}, \quad (8.7)$$

giving

$$\mathcal{S}_\nu^I(\tau) = \frac{A \mathcal{Q} u(\tau)}{\alpha_B(T_e)} \left( \frac{h^2}{2\pi m k T_e} \right)^{3/2} 2 \left( \frac{\nu}{c} \right)^2 \exp [h(\nu_1 - \nu)/kT_e] \quad (8.8)$$

(Approximation I).

We obtain  $I_\nu^d$  in Approximation II on substituting  $\mathcal{S}_\nu^I$  in (8.5). With  $T_e$  constant this gives

$$I_\nu^d(\tau, \mu) = \mathcal{S}_\nu^I(\tau) C_\nu(\tau, \mu) \quad (\text{Approximation II}) \quad (8.9)$$

where

$$C_\nu(\tau, \mu) = \frac{\exp(-f_\nu \tau / \mu)}{u(\tau)} \left\{ \int_0^\tau \exp(f_\nu \tau' / \mu) u(\tau') \frac{f_\nu}{\mu} d\tau' + \int_0^\infty \exp(-f_\nu \tau' / |\mu|) u(\tau') \frac{f_\nu}{|\mu|} d\tau' \right\} \quad (8.10)$$

and where we now consider optically thick nebulae,  $\tau_e = \infty$ . We introduce

$$X = 1 - s(\tau), \quad X' = 1 - s(\tau'). \quad (8.11)$$

Integration by parts, using  $u(\tau') = dX'/d\tau'$  (§ 4.1), gives

$$u(\tau) C_\nu(\tau, \mu) = - \int_0^\tau (X' - X) \frac{f_\nu^2}{\mu^2} \exp [f_\nu(\tau' - \tau)/\mu] d\tau' \\ + \int_0^\infty (X' + X) \frac{f_\nu^2}{\mu^2} \exp [-f_\nu(\tau + \tau')/\mu] d\tau' \quad (8.12)$$

for  $\mu > 0$  and

$$u(\tau) C_\nu(\tau, \mu) = \int_\tau^\infty (X' - X) \frac{f_\nu^2}{\mu^2} \exp [f_\nu(\tau' - \tau)/\mu] d\tau' \quad (8.13)$$

for  $\mu < 0$ . We may now carry out the integration over  $\mu$  required to obtain the mean intensity. Defining

$$C_\nu(\tau) = \frac{1}{2} \int_{-1}^1 C_\nu(\tau, \mu) d\mu, \quad (8.14)$$

we obtain

$$C_\nu(\tau) = \frac{f_\nu}{2u(\tau)} \int_0^\infty \left[ \left( \frac{X + X'}{\tau + \tau'} \right) \exp [-f_\nu(\tau + \tau')] \right. \\ \left. + \left( \frac{X - X'}{\tau - \tau'} \right) \exp (-f_\nu |\tau - \tau'|) \right] d\tau'. \quad (8.15)$$

The mean intensity of diffuse radiation, in Approximation II, is

$$J_\nu^d = \mathcal{S}_\nu^I(\tau) C_\nu(\tau). \quad (8.16)$$

Table V gives values of  $C_\nu(\tau)$  for  $T_s = 4 \times 10^4$  °K and  $2 \times 10^5$  °K.

TABLE V

		$C_\nu(\tau)$						
		$T_s = 4 \times 10^4$ °K						
$\nu/\nu_1$	$\tau$	1·000	1·082	1·104	1·292	1·651	2·000	3·000
0·0	0·0	0·77	0·74	0·73	0·65	0·51	0·40	0·20
0·1	0·1	0·82	0·78	0·77	0·69	0·54	0·43	0·21
1·0	1·0	1·00	0·99	0·98	0·93	0·78	0·64	0·33
3·0	3·0	1·09	1·13	1·14	1·21	1·25	1·17	0·72
7·0	7·0	1·07	1·10	1·11	1·27	1·79	2·21	2·03
10·0	10·0	1·03	1·05	1·06	1·18	1·83	2·71	3·33
		$T_s = 2 \times 10^5$ °K						
$\nu/\nu_1$	$\tau$	1·000	1·082	1·104	1·292	1·651	2·000	3·000
0·0	0·0	0·85	0·82	0·82	0·76	0·65	0·55	0·31
0·1	0·1	0·88	0·86	0·85	0·79	0·67	0·57	0·32
1·0	1·0	0·99	0·98	0·98	0·94	0·84	0·73	0·43
3·0	3·0	1·03	1·04	1·04	1·05	1·04	0·98	0·63
7·0	7·0	1·02	1·02	1·03	1·05	1·12	1·15	0·89
10·0	10·0	1·01	1·01	1·01	1·03	1·09	1·16	1·00

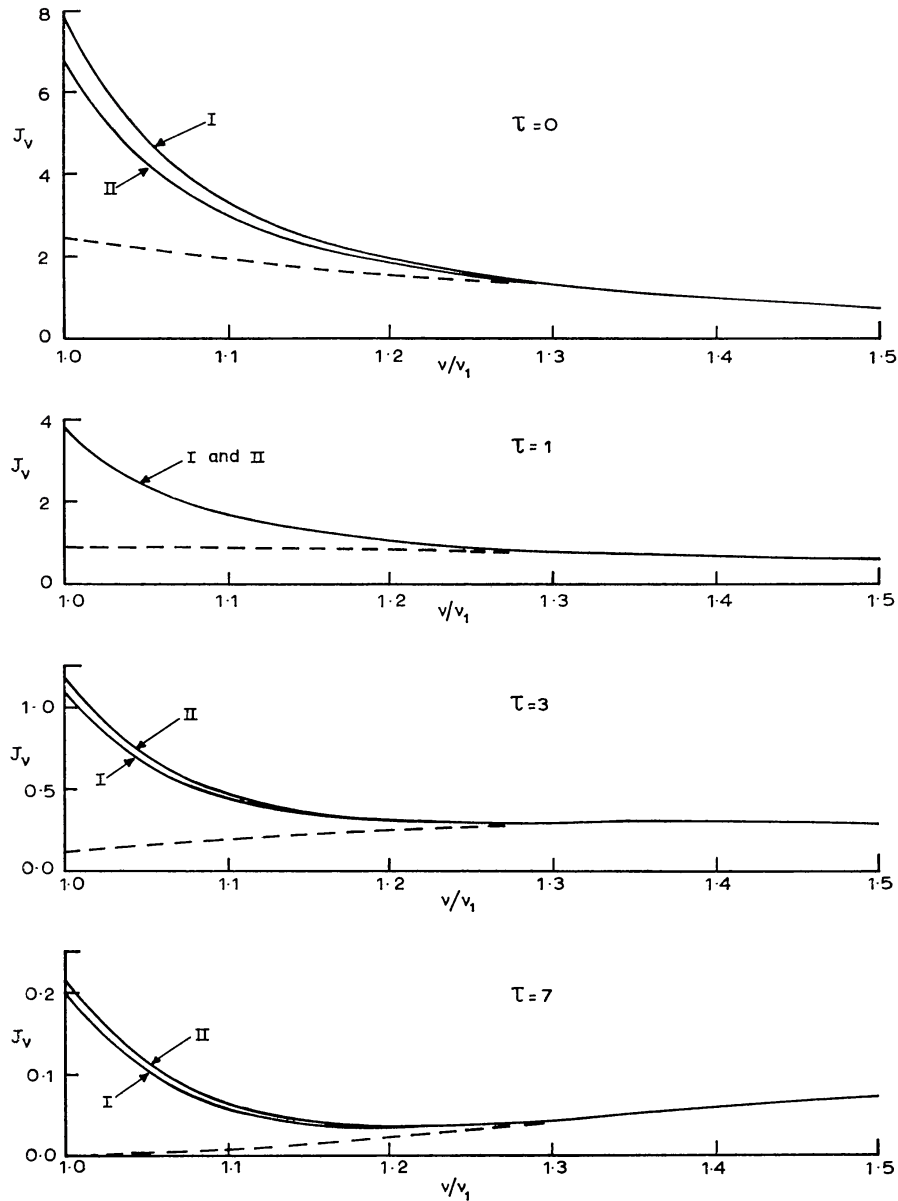


FIG. 6.—Mean intensities  $J_\nu$ , in units of  $\mathcal{Q}/4\pi\nu_1$  for  $T_s=4 \times 10^4$  °K,  $T_e=1 \times 10^4$  °K:

— — — mean intensity of attenuated stellar radiation,  $J_\nu^s$ ,  
 ————— total mean intensity in Approximations I and II.

Fig. 6 shows some results for  $T_s=4 \times 10^4$  °K,  $T_e=1 \times 10^4$  °K. The radiation intensities are given in units of  $\mathcal{Q}/4\pi\nu_1$ . In these units we have

$$J_\nu^s = \frac{h\nu_1}{kT_s} \cdot \frac{\nu^2 [\exp(\nu) - 1]^{-1} \exp(-\tau f_\nu)}{F(T_s)} \quad (8.17)$$

and, for  $T_e=1 \times 10^4$  °K,

$$\mathcal{S}_\nu^I = 10 \cdot 06 \left( \frac{\nu}{\nu_1} \right)^2 \exp \left[ 15 \cdot 789 \left( 1 - \frac{\nu}{\nu_1} \right) \right] u(\tau). \quad (8.18)$$

The total mean intensity is

$$J_\nu = J_\nu^s + \mathcal{S}_\nu^I \quad (8.19)$$

in Approximation I and

$$J_{\nu} = J_{\nu}^s + \mathcal{S}_{\nu}^I C_{\nu}(\tau) \quad (8.20)$$

in Approximation II. It is seen (Fig. 6) that the results in Approximations I and II do not differ by more than a few per cent.

*Acknowledgments.*—Much of this work was done while the first-named author held a Fulbright Scholarship (1959–1961). We would like to acknowledge the support of the United States Office of Naval Research under Contract N62558–3207 for the continuation of this research.

*Dept. of Physics,  
University College,  
London, W.C.1:  
1962 September.*

### References

- Aller, L. H., Baker, J. G., and Menzel, D. H., 1939, *Ap. J.*, **90**, 601.  
 Ambarzumian, V. A., 1932, *M.N.*, **93**, 50.  
 Axford, W. I., 1961, *Phil. Trans. Roy. Soc.*, A **253**, 301.  
 Chandrasekhar, 1935, *Zs. f. Ap.*, **9**, 266.  
 Gershberg, R. E., 1961, *Astr. Zhur.*, **38**, 250.  
 Goldsworthy, F. A., 1961a, *Progress in Aeronautical Sciences*, **1**, 174; 1961b, *Phil. Trans. Roy. Soc.*, A **253**, 277.  
 Hagihara, Y., 1938, *Jap. J. Astr. and Geophys.*, **15**, 1.  
 Hummer, D. G., 1963, *M.N.*, **125**, 461.  
 de Jong, J. H., 1951, *B.A.N.*, **11** (No. 428), 345.  
 Mathis, J. S., 1962, *Ap. J.*, **136**, 374.  
 Milne, E. A., 1924, *Phil. Mag.*, **47**, 209.  
 Pottasch, S. R., 1960, *Ap. J.*, **131**, 202.  
 Rabinowitz, P., and Weiss, G., 1959, *M.T.A.C.*, **13**, 285.  
 Seaton, M. J., 1959, *M.N.*, **119**, 81; 1960, *Reports on Progress in Physics*, **23**, 313.  
 Spitzer, L., 1948, *Ap. J.*, **107**, 6.  
 Strömgren, B., 1939, *Ap. J.*, **89**, 526.  
 Zanstra, H., 1927, *Ap. J.*, **65**, 50; 1931, *Publ. Dom. Astr. Obs. (Victoria)*, **4**, 209; 1951, *B.A.N.*, **11** (No. 428), 341.